Physica B 405 (2010) 559–563

Contents lists available at ScienceDirect

Physica B

journal homepage: www.elsevier.com/locate/physb

On barrier height inhomogeneities of Au and Cu/n-InP Schottky contacts

H. Çetin [a,*], E. Ayyildiz [b]

[a] Bozok University, Faculty of Arts and Sciences, Department of Physics, 66100 Yozgat, Turkey
[b] Erciyes University, Faculty of Arts and Sciences, Department of Physics, 38039 Kayseri, Turkey

ARTICLE INFO

Article history:
Received 29 July 2009
Received in revised form
5 September 2009
Accepted 7 September 2009

Keywords:
Schottky contact
Barrier height inhomogeneities
XPS

ABSTRACT

In this work, barrier height inhomogeneity and its origin are investigated for Au and Cu/n-InP metal/semiconductor contacts. The effective barrier height values of the Au and Cu/n-InP Schottky barrier diodes (SBDs) have been obtained as 0.480 and 0.404 eV from current–voltage (*I–V*) characteristics using the thermionic emission theory. The barrier height values of the Au and Cu/n-InP SBDs have been obtained as 0.524 and 0.453 eV from the experimental reverse bias capacitance–voltage (*C–V*) characteristics, respectively. The discrepancy between the barrier heights could be explained in terms of barrier height inhomogeneity approach. To investigate origin of the barrier height inhomogeneity, the interface atomic concentration and its distribution have been obtained by deep profile analysis using electron spectroscopy for chemical analysis (ESCA) data. The analysis shows that the interface is not abrupt. Thus, we could say lateral barrier height inhomogeneity could arise from the interface inhomogeneity.

1. Introduction

Metal–semiconductor (*MS*) contacts have great importance both in modern electronic applications and understanding solid-state electronic devices. Metal–semiconductor contacts have been specially used as gate electrodes of a field-effect transistor (MESFET), the drain and source contacts in metal-oxide-semiconductor field-effect transistor (MOSFET) which is the most important device for very-large-scale integrated circuits such as microprocessors and semiconductor memories, the electrodes for high-power IMPATT oscillators, and fabrication of photodetectors and solar cells [1–3]. The current-transport process and device technology of MS structures have been reviewed by Rhoderick [4] and by Rideout [5]. The current transport in MS contacts is mainly due to majority carriers in contrast to p–n junctions where the minority carriers are responsible. MS contacts are assumed to be abrupt junction with a fixed barrier height with respect to the classical model. The Schottky barrier height is an important parameter which determines the electrical characteristics of MS contacts and has crucial importance for successful operation of semiconductor devices [1–10]. Schottky barrier height is defined as the difference between the edge of the respective majority-carrier band of the semiconductor and the Fermi level at the interface. Most of the experimental and theoretical studies have been made on the nature and formation of the barrier height at MS contacts. It is suggested that interface states exist at the interface and these states could pin the Fermi level position at an energy level [11–13]. These states have been classified into various names such as intrinsic surface states [11], metal-induced gap states (MIGS) [12,13], and defect-related states [14,15]. Generally, the interfaces have been implicitly assumed to be laterally uniform [16–18]. The electrical requirements for a good Schottky barrier diode can be arranged in order an ideality factor approaching 1, low series resistance, and low reverse leakage currents [4,8].

The current–voltage (*I–V*) characteristics of real Schottky barrier diodes have difference from the prediction of thermionic emission theory (TET). TET assumes that the junction is abrupt with fixed Schottky barrier height (SBH) [16–18]. Furthermore, certain experimental data analyzed using TET cannot be well understood. For example, ideality factor is larger than unity and this indicates that the barrier heights change as a function of applied voltage. Another commonly observed anomaly is the dependence of SBH on the measurement technique. SBHs measured by the *C–V* technique often significantly exceed that derived from *I–V* and photo-response (*PR*) techniques. These deviations have been explained by assuming the presence of the lateral barrier height inhomogeneities [7–10,16–36]. Some common causes for the barrier heights difference have been mentioned in the literature, such as contamination in the interface, an intervening insulator layer, deep impurity levels or edge leakage currents [1–4]. Some researcher have explained the discrepancy by the existence of two regions of contact area, each having a different barrier height [20,21]. Song et al. [10] have

* Corresponding author. Tel.: +90 354 242 10 21/2580; fax +90 354 242 10 22.
E-mail address: hidayet.cetin@bozok.edu.tr (H. Çetin).

0921-4526/$ - see front matter © 2009 Elsevier B.V. All rights reserved.
doi:10.1016/j.physb.2009.09.065

reported that the difference in the SBHs obtained from *C–V* and *I–V* measurements has occurred as a result of the lateral barrier inhomogeneities. These inhomogeneities could arise from non-uniformity of the interface, defects, inhomogeneous oxide layer thickness, distribution of interfacial charges. Ballistic electron emission microscopy is a suitable method to determine the local SBH on the nanometer scale [27–29]. The spatial and statistical SBH distribution can be directly obtained by collecting many BEEM spectra measured at different locations, randomly spread over the contacts. Werner and Gütter [18] have presented analytical potential fluctuations model for the interpretation of *I–V* and *C–V* measurements on spatially inhomogeneous Schottky contacts. In their analysis, they have shown that the ideality factor n of abrupt Schottky contacts reflects the deformation of the barrier distribution under applied bias. Tung [16] has analyzed the current transport at inhomogeneities SBDs taking account on the presence of small regions with a low SBH embedded in an interface with a uniform high SBH.

In this work, the *I–V* and *C–V* characteristics of Au and Cu/n-InP (1 0 0) Schottky contacts have been measured at room temperature and determined effective barrier heights and ideality factors. We have investigated barrier height inhomogeneity and its origin by using deep profile analysis.

2. Experimental procedures

In this study, n-type unintentionally doped, having a free carrier concentration of $4.5\times10^{15}\,cm^{-3}$ and one side polished InP (1 0 0) wafers are used. Firstly, the wafer is ultrasonically cleaned with trichloroethylene, acetone and methanol for 5 min, respectively. The wafers rinse in de-ionized water of 18 MΩ and dry with high purity N_2. The native oxide on the surface of the substrate is etched in acid solution ($HF:H_2O=1:10$) for 60 s. Again, rinse in de-ionized water of 18 MΩ and dry with high purity N_2. After the etching process, the wafer is immediately inserted into the deposition chamber. Ohmic contacts are made by evaporation of In on nonpolished side of the InP wafer and then by thermal annealing at 350 °C for 60 s in flowing nitrogen in a quartz tube furnace. The circular shaped Schottky metals, Au and Cu are then deposited through a Mo mask by thermal evaporation. Schottky metal thickness (240 Å) is monitored using a quartz oscillator. The pressure during evaporation is at about 10^{-6} mbar. The current–voltage (*I–V*) and capacitance–voltage (*C–V*) characteristics of the Au and Cu/n-InP Schottky barrier diodes have been measured using a HP 4140B picoamperemeter and a HP 4280A 1 MHz C meter, respectively, at room temperature. Deep profile analysis obtained from Schottky metal surface to the substrate by using ESCA with equipped ion bombardment unit. After each ion bombardment, the spectrum obtained by X-ray photoelectron emission spectroscopy (XPS) is taken from the shaved surface.

3. Experimental results and discussion

3.1. The I–V and C–V characteristics of the Schottky barrier diodes

One of the most widely used methods to determine the SBH of a metal–semiconductor contact is the current–voltage measurement. In a moderately doped semiconductor, the current I across a Schottky barrier diode under bias voltage V with the zero-bias effective barrier height $q\Phi_{b0}^{eff}$ is usually described by the thermionic emission theory [2,4]

$$I = I_0\exp\left(\frac{qV}{nkT}\right)\left[1-\exp\left(-\frac{q(V-IR_s)}{kT}\right)\right] \quad (1)$$

where R_s is the series resistance, I_0 is the saturation current which is determined by

$$I_0 = AA^*T^2\exp\left(\frac{-q\Phi_{b0}^{eff}}{kT}\right) \quad (2)$$

where A is the area of the diode which is effective for current transport, A^* is the effective Richardson constant and equal $9.24\,A\,cm^{-2}\,K^{-2}$ for n-type InP [3], T is the measuring temperature in absolute scale, k is the Boltzmann constant, q is the elementary charge, $q\Phi_{b0}^{eff}$ is the effective barrier height obtained from the extrapolation of I_0 in the semi-log forward bias $\ln I$–V characteristics according to [2,4]

$$q\Phi_{b0}^{eff} = kT\ln\left(\frac{A^*AT^2}{I_o}\right) \quad (3)$$

and n is the ideality factor which should be $n=1$ for an ideal diode. The values of n are calculated from the slope of the linear regions of the forward *I–V* characteristics according to [2,4]

$$n = \frac{q}{kT}\frac{dV}{d(\ln I)} \quad (4)$$

Fig. 1 shows the room temperature experimental semilog-forward and reverse bias *I–V* characteristics of the Au/n-InP and Cu/n-InP Schottky barrier diodes, respectively. From the slope of the *I–V* curves, the ideality factors have been obtained as 1.04 and 1.06 for the Au and Cu/n-InP SBDs, respectively. It is well known that the nearly ideal diode *I–V* characteristic in the forward bias has with near-unity ideality factor and reverse bias has the near-voltage independent saturation currents. The values of barrier heights for the Au and Cu/n-InP *SBDs* have been calculated as 0.480 and 0.404 eV, respectively; and these values agree with the literature [37]. Idealities greater than unity have been ascribed to several effects; interfaces states at a thin oxide which exists between the metal and the semiconductor [4,18,38], tunneling currents in highly doped semiconductors and generation-recombination currents in the space-charge region [2,4]. These models describe

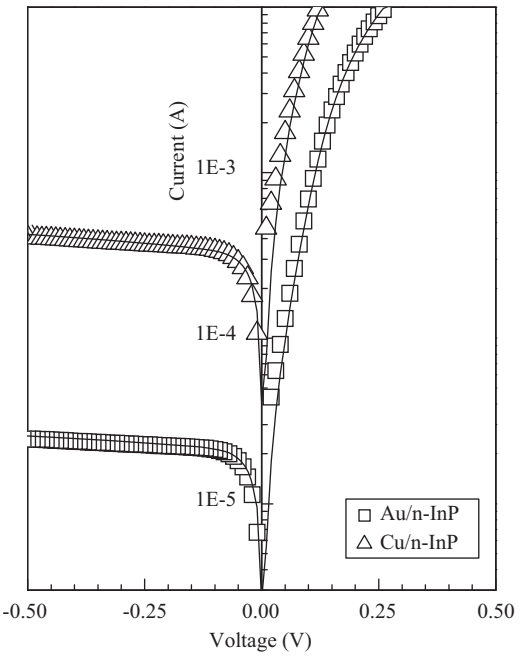

Fig. 1. The experimental semi-log forward and reverse bias current–voltage characteristics of the Au and Cu/n-InP Schottky barrier diodes at room temperature (triangle and square shapes). The full lines indicate least squares fits of Eq. (9) to the experimental data.

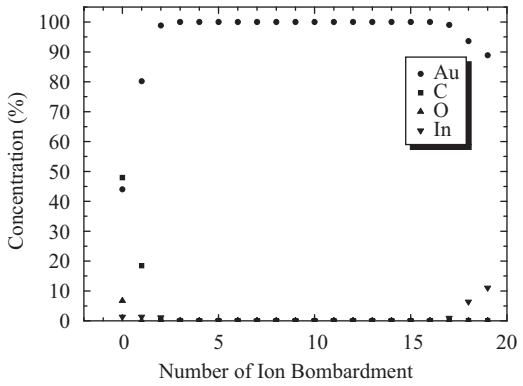

Fig. 2. The deep profile analysis obtained from Schottly metal for the Au/n-InP diode.

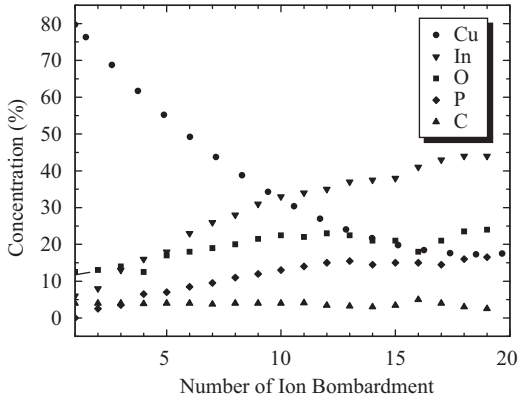

Fig. 3. The deep profile analysis obtained from Schottky metal for the Cu/n-InP diode.

extreme cases of Schottky contacts (interfacial layer, high doping, traps in the space-charge region), and all of them tacitly assume a spatially homogeneous atomically flat interface between the metal and semiconductor, as pointed out in the literature [2,4,18]. Furthermore, when a metal is evaporated on a chemically cleaned semiconductor, the metal and semiconductor are not intimate contact. At the contact region, diffusion and exchange may occur depending on the sort of semiconductor and metal. Figs. 2 and 3 show atomic concentrations which is obtained from Au and Cu Schottky metal surfaces by using ESCA with equipped ion bombardment unit, respectively. The atomic concentrations have been calculated from X-ray photoemission spectra obtained after each ion bombardment. After each bombardment, Schottky metal surface is shaved by ion bombardment and XPS spectrum is obtained new, shaved surface. This could supply information about atomic concentration distribution from metal surface to the crystal substrate. In Fig. 2, it can be seen that Au diffuses into InP at the contact region and In diffuse into Au Schottky metal. In Fig. 3, In and P diffusion into Cu Schottky metal could be clearly seen. Although all evaporation processes are made under 10^{-5} Torr, there is oxide species especially in Fig. 3. Furthermore, few dose C pollution could be seen in the graph. The figures mean each evaporated metal interact with the InP substrate separately and there are not abrupt interfaces. Because In and P diffusion to the Schottky metal have been different, different type interface shape are formed. Furthermore, the atomic diffusion cannot be completely homogeneous at the lateral distances on the Schottky metal surface. Firstly, laterally inhomogeneous atomic exchange and diffusion can constitute laterally inhomogeneous barrier height.

Most frequently semiconductor surface is prepared by chemical etching and this invariably produce thin oxide layer of thickness about 10–20 Å [4]. Our chemically cleaned InP substrate has about 20 Å oxide thickness measured by elipsometry. The precise nature and thickness of the oxide layer depend on the exact method of the surface preparing [28]. There is inevitably a thin interfacial layer between the metal and semiconductor. Then, a thin interfacial layer is present even in InP Schottky barrier diodes without any intentional interfacial layer [39]. Interfacial oxide layer can include various oxide species [38]. Secondly, inhomogeneous interfacial oxide layer thickness and oxide species can cause laterally inhomogeneous barrier height.

The SBH can also be determined by the capacitance–voltage (C–V) measurements. In Schottky diodes, the depletion layer capacitance can be expressed as [2,4]

$$C^{-2} = 2(V_{do} + V)/q\varepsilon_s A^2 N_d \tag{5}$$

where A is the area of the diode, V_{d0} is the diffusion potential at zero bias and is determined from the extrapolation of the linear C^{-2}–V plot to the V axis, N_d is the doping concentration in the substrate, ε_s is the permittivity of the semiconductor. The value of the barrier height can be obtained by the relation [2,4]

$$q\Phi_b(C-V) = qV_{d0} + qV_n + kT \tag{6}$$

where V_n is the potential difference between the Fermi level and the bottom of the conduction band at the neutral region. V_n can be calculated from the following relation

$$V_n = \left(\frac{kT}{q}\right)\ln\left(\frac{N_c}{N_d}\right) \tag{7}$$

where N_c=4.93 × 10^{17} cm^{-3} is the effective density of states in the conduction band for the InP semiconductor [9].

Fig. 4 shows the reverse bias C^{-2}–V curves of the Au and Cu/n-InP SBDs at frequency of 1.0 MHz. Because interface states could not follow this frequency range, interface states effects on the C–V measurements can be ignored. As can be seen from Eq. (5), the C^{-2}–V plot is a straight line where the intercept with the V axis gives the values of V_{d0}. The linearity of the plot indicates a uniform doping distribution. The value of 0.388 V for the diffusion potential and the doping concentration of 7.25 × 10^{15} cm^{-3} have been obtained for the Au/n-InP SBD, respectively. Furthermore, the diffusion potential and the doping concentration values have been obtained 0.328 V and 10.68 × 10^{15} cm^{-3} for the Cu/n-InP SBD. Thus, the barrier height values of 0.524 and 0.453 eV are determined using the above doping concentrations and V_n values

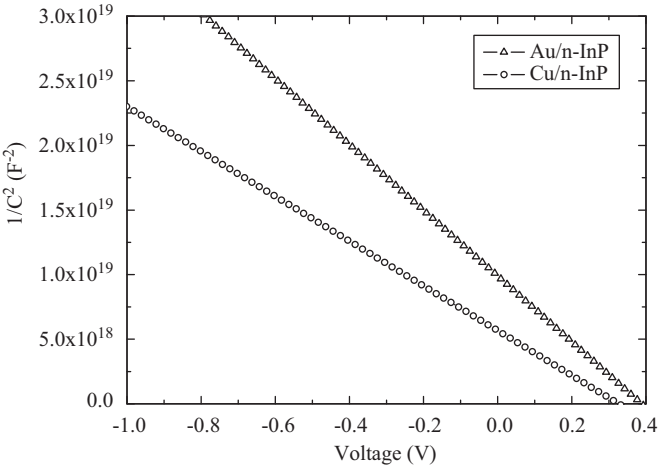

Fig. 4. The reverse bias C^{-2}–V characteristics of the Au and Cu/n-InP Schottky barrier diodes at room temperature and 1 MHz.

of 0.109 and 0.099 V for the Au and Cu/n-InP SBDs, respectively. As can be seen, the barrier height values obtained from the reverse bias C^{-2}–V characteristics are different that of obtained from the I–V characteristics. The differences were 0.044, 0.049 eV for the Au and Cu/n-InP SBDs, respectively. For uniform MS contacts, it has been found that the intercept of the voltage axis in a plot of C^{-2} versus V gives the barrier height of the MS contact less V_n, in good agreement with the SBH obtained by the I–V characteristics. This difference for both of the diodes may be explained by existence of SBH inhomogeneity on MS contacts [16–36], as will discuss below.

3.2. Schottky barrier inhomogeneity model

Abnormal experimental results such as ideality factor greater than unity and the dependence of barrier height on the technique of measurement can be attributed to the existence of barrier height inhomogeneities [16–36]. There are two different approaches which explained the inhomogeneity. One approach assumes a continuous spatial distribution of SBH and the total current across a Schottky diode is simply calculated by integrating the current determined by the ideal TE model with an individual barrier height and weighted by the distribution function (parallel-conduction model) [18–26]. Using the accepted Gaussian distribution; the total current is described approximately by an analytical expression similar to the TE theory with an apparent barrier height and an apparent ideality factor. The other approach, one assumes that some small patches of low SBH are embedded in the uniform higher SBH regions [16,17,30–36]. The conduction path in front of a small patch with a low SBH is pinched off if surrounded by the presence of high-SBH regions in its close proximity when the size of the patches becomes comparable to or are smaller than the depletion layer width (w) [16]. When pinch-off occurs, the barrier at a saddle point in front of the low-SBH area determines the transport properties. The condition for pinch-off is given by [16]

$$\frac{\Delta}{V_{bb}} > \frac{2R_p}{w} \tag{8}$$

where Δ, V_{bb}, R_p are the barrier height reduction at the interface of the patch compared to the homogeneous value, the interface band bending of the uniform barrier outside the patches, the radius of a circular patch, respectively. Of course, as Δ approaches zero, the potential profiles become identical to those of a MS contact with uniform SBH. The barrier height at the saddle point is intermediate between the values of the patch itself and of the surrounding homogeneous contact area [16]. The total current through the inhomogeneous MS contact which exhibit circular patches with Gaussian distribution of the patch parameter $\gamma = (3(R_p^2\Delta/4)^{1/3})$ is given by [16,34]

$$I = AA^*T^2 \exp\left(\frac{\Phi_b^{\text{hom}}}{kT}\right)\left[\exp\left(\frac{q(V-IR_s)}{kT}\right)-1\right](1+P) \tag{9}$$

$$I = I_{te}^{\text{hom}}(1+P) \tag{10}$$

the total current is composed of the current through the whole area with a uniform SBH Φ_b^{hom}, a homogeneous Schottky contact area A, series resistance R_s and the current through the patches. The patch function P which describes the modification of the I–V plot due to the patches can be written by [16,34]

$$P = \frac{8\pi\rho_p\sigma^2\eta^{1/3}}{9(V_{b0}-V+IR_s)^{1/3}} \exp\left[\frac{q^2\sigma^2(V_{b0}-V+IR_s)^{2/3}}{2(kT)^2\eta^{2/3}}\right] \tag{11}$$

where σ is standard deviation of $\gamma \geq 0$, V_{b0} is the band bending of the uniform barrier at zero bias, and $\eta = \varepsilon_s\varepsilon_0/qN_d$ where ε_0, ε_s are the dielectric constant of the free space and the semiconductor, respectively.

Fig. 1 shows the experimental semi-log forward and reverse bias current–voltage characteristics of the Au and Cu/n-InP Schottky barrier diodes (the full lines) at room temperature and least-square fits of Eq. (9) to experimental data. The fitting parameters are the homogeneous barrier height Φ_b^{hom}, the standard deviation σ_p of the patch parameter γ_p, the area density of the patch ρ_p and the series resistance R_s. As can be seen from Fig. 1, there is excellent agreement between the experimental data and the fitted curves. This means that the experimental data are very well described by the pinch-off theory of Tung. We have obtained a homogeneous barrier height $\Phi_b^{\text{hom}} = 0.506$ eV, a standard deviation of the patch parameter $\sigma_p = 4.90 \times 10^{-5}$ cm$^{2/3}$ V$^{1/3}$, a patch density $\rho_p = 25.0 \times 10^9$ cm^{-2}, a series resistance $R_s = 10\,\Omega$ by using $N_d = 7.25 \times 10^{15}$ cm^{-3}, $V_{b0} = 0.388$ V, $A = 7.85 \times 10^{-3}$ cm^2 and $T = 296$ K for the Au/n-InP SBD. In addition to, we have obtained a homogeneous barrier height $\Phi_b^{\text{hom}} = 0.434$ eV, a standard deviation of the patch parameter $\sigma_p = 4.85 \times 10^{-5}$ cm$^{2/3}$ V$^{1/3}$, a patch density $\rho_p = 10.5 \times 10^9$ cm^{-2}, a series resistance $R_s = 3\,\Omega$ by using $N_d = 10.68 \times 10^{15}$ cm^{-3}, $V_{b0} = 0.328$ V, $A = 7.85 \times 10^{-3}$ cm^2 and $T = 296$ K for the Cu/n-InP SBD. The difference between the homogeneous and effective barrier heights of the Au/n-InP SBD is $\Phi_b^{\text{hom}} - \Phi_{b0}^{eff} = 0.026$ eV. This difference for the Cu/n-InP SBD is $\Phi_b^{\text{hom}} - \Phi_{b0}^{eff} = 0.030$ eV. It has been observed that these values are very close to each other. The combined effect of all the low SBH patches is as if there were a big low SBH region in the diode with an effective area of ρAA_{eff} and an effective Φ_{eff} SBH (both of which are dependent on the patch parameter γ) [16]. Furthermore, the effective area of the low SBH patch is given by [16]

$$A_{eff} = \frac{8\pi\sigma^2}{9}\left(\frac{\eta}{V_{b0}}\right)^{1/3} \tag{12}$$

The patch radius R_p is found to be 9.56 nm for the Au/n-InP SBD using the fitting parameters and Eq. (12). This value is 28.34 times lower than the depletion layer width, $w = 2.71 \times 10^{-5}$ cm.

For a current described by Eq. (9), the ideality factor is given by [16]

$$n \approx 1 + \Delta n, \quad \Delta n \approx \frac{\sigma^2 V_{b0}^{-1/3}}{3kT\eta^{2/3}} \tag{13}$$

Furthermore, the value of $n = 1.04$ from the fitting the parameters is the same as the value of 1.04 obtained from the experimental I–V characteristics for the Au/n-InP SBD.

Again, the patch radius R_p is found to be 9.12 nm for the Cu/n-InP SBD using the fitting parameters and Eq. (12). This value is 22.48 times lower than the depletion layer width $w = 2.05 \times 10^{-5}$ cm and the value of $n = 1.06$ from the fitting the parameters is the same as the value of 1.06 obtained from the experimental I–V characteristics for the Cu/n-InP SBD.

Im et al. [29] have reported a simultaneous microscopic and macroscopic test of the Tung model of SBH inhomogeneity as applied to metal/6H-SiC SBDs, by measuring the nm-scale barrier height distribution of particular SBDs using ultra-high vacuum ballistic electron emission microscopy (BEEM). Anand et al. [31] have investigated of electron transport at the Au/n-InP MS interface in the presence of nanoscopic barrier inhomogeneities. To realize this, they have fabricated a composite MS structure comprising a known density of nanometer sized Ag aerosol particles on InP overlayed by a uniform Au film. The main purpose of using a composite structure is to deliberately introduce inhomogeneties such that the spatial variation of the barrier height is on a scale comparable to the depletion width. For, the observed barrier height inhomogeneity, the SB formation mechanism has been sensitive to local parameter at a MS interface.

Furthermore, numerical simulations have shown that as the low SBH patch radius decrease, the patches become more pinched-off (i.e. the potential at the saddle point increases). At some critical patch size, there is no pinch-off, and patches much larger than the critical size. The potential distribution approaches that of a uniform MS contact with the same SBH as that of the low SBH patch [17]. Experimentally observed SBHs have been often an average over a wide range of different FL positions which caused by fluctuating local parameters.

Numerical simulations of the inhomogeneous MS contacts [17] have shown that their flat-band barrier heights are close to the weighted arithmetic average of their local SBHs. The reason for the discrepancy between the SBHs obtained from *I–V* and *C–V* characteristics is clear. The current in the *I–V* measurement is dominated by the current which flows through the region of low SBH. Since the low-SBH patch is pinched-off, the effective SBH of the patch is the potential at the saddle point. The flat-band barrier heights Φ_b^{CV} of Schottky contacts with low-SBH patches are equal to their homogeneous barrier heights Φ_b^{hom} plus image-force lowering $\delta\Phi_b^{if}$ both at zero bias [9].

The barrier lowering due to the image-force at the MS contacts [2,4] is given by

$$\Delta\Phi_{im} = \left\{ \frac{q^3 N_d}{8\pi^2 \varepsilon_0^3 \varepsilon_s^3} \left(\Phi - V_n - \frac{kT}{q} \right) \right\}^{1/4} \tag{14}$$

where the terms have their usual meaning. The values of the image-force lowering have been found to be 0.018 and 0.019 eV from Eq. (13) Au and Cu/n-InP SBDs, respectively. For the Au/n-InP SBD, the difference between the homogeneous SBH obtained from the *I–V* characteristics and the flat-band barrier height obtained from the C^{-2}-*V* characteristics is 0.018 eV. This value agrees with $\Delta\Phi_{im}$ (Au). Again, the difference between the homogeneous SBH and the flat-band barrier height is 0.019 eV for the Cu/n-InP SBD. This value also agrees with $\Delta\Phi_{im}$ (Cu). The true formation mechanism of the SBH seems to be the one that determines the local FL position based on the local specifics of the MS interface, as reported in Refs. [9,18].

4. Conclusions

We have investigated barrier height inhomogeneities of the Au and Cu/n-InP SBDs fabricated by evaporation of Au and Cu films on the chemically etched n-InP substrate. The forward *I–V* characteristics of the devices have been analyzed in terms of the thermionic emission model. The barrier height values are obtained as 0.480 and 0.404 eV for the Au and Cu/n-InP SBDs, respectively. The values of 0.524 and 0.453 eV for barrier heights of the Au and Cu/n-InP SBDs are obtained from the experimental reverse bias capacitance–voltage (*C–V*) characteristics, respectively. The discrepancy between the barrier heights determined from *I–V* and *C–V* may be explained in terms of inhomogeneity SBH approach. As could be seen in the deep profile analysis, the interface could not be abrupt as a result of interactions and diffusions. Thus, the lateral inhomogeneity could arise from metal and semiconductor interactions, reactions and atomic diffusion.

Schottky barrier diodes have been interpreted on the basis of Tung's theoretical model which assumes the existence of barrier height inhomogeneity at the metal–semiconductor interface. Our results show that the electron transport at the metal/semiconductor contacts are significantly affected by low-barrier regions, as pointed out Tung and co-worker [16,17]. The homogeneous barrier heights of the Au and Cu/n-InP SBDs were found to be 0.506 and 0.434 eV, respectively. Furthermore, the flat-band barrier heights Φ_b^{CV} of Schottky contacts with low-SBH patch are equal to their homogeneous barrier heights Φ_b^{hom} plus image-force lowering $\delta\Phi_b^{if}$ both at zero bias.

Acknowledgment

This work has been supported by the Scientific Research Project Unit of Erciyes University through Project no. 02–012–11 EÜBAP.

References

[1] R.T. Tung, Mater. Sci. Eng. R 35 (2001) 1.
[2] S.M. Sze, Physics of Semiconductor Devices, Wiley, New York, 1981.
[3] C.W. Wilmsen, Physics and Chemistry of III–V Compound Semiconductor Interfaces, Plenum Press, New York, 1985.
[4] E.H. Rhoderick, Metal–Semiconductor Contacts, Oxford, Clarendon, 1978.
[5] L. Rideout, Thin Solid Films 48 (1978) 261.
[6] Z.S. Horváth, J. Vac. 46 (1995) 963.
[7] B. Boyarbay, H. Çetin, M. Kaya, E. Ayyildiz, Microelectron. Eng. 85 (2008) 721.
[8] L.J. Brillson, Contacts to the Semiconductor, Noyes, New Jersey, 1993.
[9] W. Mönch, Semiconductor Surfaces and Interfaces, Springer, Berlin, 1995.
[10] Y.P. Song, R.L. Van Meirhaeghe, W.H. Laflere, F. Cardon, Solid-State Electron. 29 (1986) 633.
[11] J. Bardeen, Phys. Rev. 71 (1947) 717.
[12] V. Heine, Phys. Rev. A 138 (1965) 1689.
[13] J. Tersoff, Phys. Rev. Lett. 52 (1984) 465.
[14] W.E. Spicer, I. Lindau, P. Skeath, C.Y. Su, J. Vac. Sci. Technol. 17 (1980) 1019.
[15] H. Hasegawa, T. Sato, C. Kaneshiro, J. Vac. Sci. Technol. B 17 (1999) 1856; H. Hasegawa, H. Ohno, J. Vac. Sci. Technol. B 4 (1986) 1130.
[16] R.T. Tung, Phys. Rev. B 45 (1992) 13509.
[17] R.T. Tung, A.F.J. Levi, J.P. Sullivan, F. Schrey, Phys. Rev. Lett. 66 (1991) 72; J.P. Sullivan, R.T. Tung, M.R. Pinto, W.R. Graham, J. Appl. Phys. 70 (1991) 7403.
[18] J.H. Werner, H.H. Güttler, J. Appl. Phys. 69 (1991) 1522.
[19] G.D. Mahan, J. Appl. Phys. 55 (1984) 980.
[20] I. Ohdomari, H. Aochi, Phys. Rev. B 35 (1987) 632.
[21] J.L. Freeouf, T.N. Jackson, S.E. Laux, J.M. Woodall, J. Vac. Sci. Technol. 21 (1982) 570.
[22] S. Chand, Semicond. Sci. Technol. 17 (2002) 36; S. Chand, J. Kumar, Semicond. Sci. Technol. 12 (1997) 899.
[23] P.G. McCafferty, A. Sellali, P. Dawson, H. Elabd, Solid-State Electron. 39 (1996) 583.
[24] H. Çetin, E. Ayyildiz, Semicond. Sci. Technol. 20 (2005) 625; H. Çetin, B. Şahin, E. Ayyildiz, A. Türüt, Physica B 364 (2005) 133.
[25] Ö. Güllü, M. Biber, S. Duman, A. Türüt, Appl. Surf. Sci. 253 (2007) 7246; M. Enver, A. Türüt, J. Appl. Phys. 102 (2007) 043701.
[26] I. Dökme, Ş. Altindal, M.M. Bülbül, Appl. Surf. Sci. 252 (2006) 7749.
[27] W.J. Kaiser, L.D. Bell, Phys. Rev. Lett. 60 (1988) 1406.
[28] R.L. Detavernier, V. Meirhaeghe, R. Donaton, K. Maex, F. Cardon, J. Appl. Phys. 84 (1998) 3226.
[29] H.J. Im, Y. Ding, J.P. Pelz, W.J. Choyke, Phys. Rev. B 64 (2001) 07531.
[30] S. Zu, C. Detavernier, R.L. Van Meirhaeghe, X. Qu, G. Ru, F. Cardon, B. Li, Semicond. Sci. Technol. 15 (2000) 349.
[31] S. Anand, S-B. Carlsson, K. Deppert, L. Montelius, L. Samuelson, J. Vac. Sci. Technol. B 14 (1996) 2794.
[32] R.F.K. Schmitsdorf, T.U. ampen, W. Mönch, J. Vac. Sci. Technol. B 15 (1997) 1221; R.F. Schmitsdorf, W. Mönch, Eur. Phys. J. B 7 (1999) 457.
[33] F.E. Jones, C. Daniels-Hafer, B.P. Wood, R.G. Danner, M.C. Lonergan, J. Appl. Phys. 90 (2001) 1001.
[34] H. Dogan, N. Yıldırım, A. Türüt, M. Biber, E. Ayyildiz, Ç. Nuhoglu, Semicond. Sci. Technol. 21 (2006) 822.
[35] W.P. Leroy, K. Opsomer, S. Forment, R.L. Van Meirhaeghe, Solid-State Electron. 49 (2005) 878.
[36] A.F. Hamida, Z. Ouennoughi, A. Sellali, R. Weiss, H. Ryssel, Semicond. Sci. Technol. 23 (2008) 45005.
[37] N. Newman, T. Kendelewicz, L. Bowman, W.E. Spicer, App. Phys. Lett. 46 (1985) 1176.
[38] H. Çetin, E. Ayyildiz, A. Türüt, J. Vac. Sci. Technol. B 23 (2005) 2436.
[39] H. Çetin, E. Ayyildiz, Appl. Surf. Sci. 253 (2007) 5961.